Neuromuscular Disorders 50 (2025) 105345

Contents lists available at ScienceDirect

Neuromuscular Disorders

journal homepage: www.elsevier.com/locate/nmd

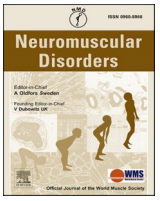

Therapeutic sphingosine-1-phosphate receptor modulation by repurposing fingolimod (FTY720) leads to mitigated neuropathy and improved clinical outcome in a mouse model for Charcot-Marie-Tooth 1X disease

Xidi Yuan [a,b,#], Dennis Klein [a,#,*], Anna-Maria Maier [a], Rudolf Martini [a]

[a] Department of Neurology, Developmental Neurobiology, University Hospital Würzburg, Würzburg, Germany
[b] Biomedical Center (BMC), Biochemistry, Faculty of Medicine, LMU Munich; Neuroimmunology and Neurodegenerative Diseases, German Center for Neurodegenerative Diseases (DZNE); Munich Cluster for Systems Neurology (SyNergy), Munich, Germany

ARTICLE INFO

Keywords:
Inherited peripheral neuropathy
Fingolimod
FTY720
Myelin
Axon damage
T-lymphocytes
Macrophages
Neuroinflammation

ABSTRACT

Previous studies have shown that both the innate and adaptive immune systems foster progression of neuropathy and clinical symptoms in a mouse model for Charcot-Marie-Tooth 1X disease. Here we demonstrate a possible therapeutic translation of these findings using the clinically approved sphingosine-1-phosphate receptor modulator fingolimod (FTY720) in *connexin32*-deficient mice mimicking Charcot-Marie-Tooth 1X disease.

Treatment with FTY720 prevented an increase of CD8+ and CD4+ T-lymphocyte numbers in both femoral quadriceps nerve as well as in ventral spinal roots. While macrophages of ventral spinal roots show a similar, albeit non-significant trend, macrophages from quadriceps nerve are not reduced upon treatment. On the histopathological level, axonopathic changes were reduced in ventral spinal roots, but not in quadriceps nerves upon treatment. Electrophysiological recordings displayed improved nerve conduction parameters upon FTY720 treatment, while clinically, FTY720 treatment ameliorated distinct parameters of motor performance and grip strength. We suggest that targeting the adaptive immune system might be a pharmacological treatment option for mitigating disease burden particularly in severe cases of Charcot-Marie-Tooth 1X.

1. Introduction

Charcot-Marie-Tooth type 1 (CMT1) diseases are genetically caused neuropathies of the peripheral nervous system (PNS) with generally poor treatment options. Since at least three CMT1 forms are driven or aggravated by neuroinflammation, dampening the immune response might be instrumental for mitigating disease progress of the primarily genetic neuropathies [1,2]. Indeed, we previously demonstrated that targeting nerve macrophages with the CSF-1 receptor inhibitor PLX5622 improved disease outcome in distinct CMT models, particularly when applied early in disease course [3–5]. Of note, in mouse models for CMT1X, the X-linked, dominant form of CMTs, the adaptive immune system appears to be another disease amplifier besides the innate immune system during progression of the neuropathy [1,6,7]. This observation may open the possibility of the therapeutic use of the sphingosine-1-phosphate receptor (S1PR) modulator fingolimod (FTY720), which impairs lymphocyte egress from secondary lymphatic organs [8], to mitigate the neuropathy. Importantly, FTY720 is clinically approved for treatment of relapsing-remitting multiple sclerosis, a neuroinflammatory disease of the central nervous system (CNS) [8–10], hence possible risks and side effects are well known. Furthermore, this immune modulator improved histopathological and clinical outcome in models for distinct genetic disorders of the CNS [11–14]. Here, we tested the possibility that repurposing the clinically approved drug FTY720 might be an option to treat CMT1X neuropathy by modulating the adaptive immune system in an appropriate mouse model. We found that S1PR-modulation in a model for CMT1X led to an amelioration of axonopathic features and to an improved clinical outcome. Thus, targeting the adaptive immune system might be an option to treat CMT1X particularly in severe, inflammation-dominated cases.

* Corresponding author.
E-mail address: Klein_D2@ukw.de (D. Klein).
shared first authorship.

https://doi.org/10.1016/j.nmd.2025.105345
Received 8 January 2025; Received in revised form 24 March 2025; Accepted 24 March 2025
Available online 25 March 2025

2. Material and methods

2.1. Mice

Cx32def [15,16] and wild-type (Cx32wt) mice of both sexes were investigated at 12 months of age (for details see below). In Cx32def mice, no sex-related differences were observed in the investigated parameters, consistent with previous reports [17,18]. All animals were bred on a C57Bl/6 J background. All animals were kept in individually ventilated cages in the animal facility at the Center of Experimental Molecular Medicine (University of Würzburg) with a 14h/10h day/night rhythm (<300 lx during day) under barrier conditions. Mice were given free access to food and water at all times. Genotyping was accomplished by conventional PCR with the use of isolated DNA from mouse tissues based on previously published PCR protocols [7]. All animal experiments were approved by the local authority of the Government of Lower Franconia, Germany.

2.2. Fingolimod (FTY720) treatment

Fingolimod (from here onwards designated as FTY720 throughout the manuscript; Sigma-Aldrich, SML0700) was administered in Cx32def mice by dissolving in autoclaved drinking water at 3 μg/mL and provided *ad libitum*. With an average body weight of 30 g and an estimated daily water consumption of 5 mL, this corresponds to the dosage of 0.5 mg/kg/day. Cx32def mice provided with autoclaved water without FTY720 were used as controls. Mice were treated from 3 months of age until 12 months of age and were weekly monitored. No adverse effect of the treatment was observed during the observation period of 9 months.

2.3. Nerve dissection and tissue processing

Animals were sacrificed by asphyxiation (CO_2) in accordance with guidelines by the State Office of Health and Social Affairs, Berlin as previously published [4]. Mice were then perfused transcardially using phosphate-buffered saline (PBS) containing heparin. To harvest fresh frozen tissue for immunohistochemistry, femoral nerves and spinal roots of Cx32def mutants and WT mice were embedded in Tissue-Tek® O.C.T. compound (Sakura) and frozen in liquid nitrogen cooled methyl butane. Fresh frozen tissues were then cut into 10-μm-thick cross-sections using a cryostat (Leica) and stored at –20 °C until further analysis.

For electron microscopy, mice were transcardially perfused with 4 % PFA and 2 % glutaraldehyde in 0.1 M cacodylate buffer for 10 min. Dissected femoral nerves and spinal roots (L3-L5) were subsequently post-fixed in the same solution overnight at 4 °C. Osmification was performed with 2 % osmium tetroxide in 0.1 M cacodylate buffer for 2 h, followed by dehydration in ascending acetone concentrations. Nerves were embedded in Spurr's medium. Ultrathin sections (70 nm) were cut and mounted to copper grids and counterstained with lead citrate.

2.4. Immunohistochemistry

Quantification of endoneurial macrophages was performed on femoral quadriceps nerve cross sections according to previously published protocols [4]. Briefly, samples were blocked with 5 % bovine serum albumin (BSA) in PBS and then incubated at 4 °C with an antibody against the pan-macrophage marker F4/80 (rat, 1:300, MCAP497, Serotec) in 1 % BSA in PBS overnight. After washing with PBS, samples were incubated with Cy3-conjugated goat anti-rat IgG (1:300, 112–165–167, Dianova) secondary antibodies for 1 h at room temperature. Nuclei were stained with DAPI (Sigma Aldrich) and slides were mounted with Aqua-Poly/Mount (Polysciences) and stored at 4 °C until further analysis. From seven to ten consecutive sections per animal, the mean numbers of F4/80-positive cells per section were determined.

Quantification of CD4+ and CD8+ lymphocytes were performed on cross sections of femoral quadriceps nerves. Samples were post-fixed in ice-cold acetone for 10 min, and then blocked with 5 % BSA in PBS. Incubation of respective primary antibodies (rat anti-CD4, 1:1000, Bio-Rad AbD Serotec; rat anti-CD8, 1:500, Bio-Rad AbD Serotec) was done overnight at 4 °C. The corresponding immune reaction was visualized using a fluorescently-labeled secondary antibody (donkey anti-rat IgG Cy3, 1:300, Dianova).

Opposed to femoral quadriceps nerves, numbers of T-lymphocytes and F4/80-positive macrophages in ventral roots are presented as cells/mm^2 due to variabilities in fiber numbers and size of spinal roots (L3-L5).

Digital fluorescence microscopic images were acquired using an Axiophot 2 microscope (Zeiss) equipped with a CCD camera (Visitron Systems). Images were minimally processed for generation of figures using Photoshop CS6 (Adobe) or Fiji/Image J (National Institutes of Health).

2.5. Morphological analysis by electron microscopy

Electron microscopic images were taken using a ProScan Slow Scan CCD camera mounted to a Leo 906E electron microscope (Carl Zeiss). Multiple images were aligned with iTEM software (Olympus Soft Imaging Solutions) to analyze complete nerve cross sections. Pathological alterations were quantified in relation to the total number of axons in corresponding cross sections of the femoral quadriceps nerve (mean axon count ~550 axons/sample) and ventral roots (mean axon count ~680 axons/sample). De- and thinly myelinated axons, degenerating or degenerated axons, Büngner bands and periaxonal vacuoles were determined and then quantified. Additionally, phagocytosing macrophages were counted, and their numbers were given as relative values per 100 axons within the nerve. Representative micrographs of indicated pathological features have been previously published [19–21].

2.6. Nerve conduction studies

Mice were anesthetized by an intraperitoneal injection with a mixture of Ketavet (Pfizer) and Xylavet (CP-Pharma) (100 mg Ketavet and 6.7 mg Xylavet per kilogram body weight) and placed under a heating lamp to avoid hypothermia. Body temperature of mice was controlled before and after measurements (34–36 °C). Neurological properties of the left sciatic nerve were measured as described previously [3,22]. Shortly, after supramaximal stimulation of the tibial nerve with monopolar needle electrodes at the ankle (distal) and the sciatic nerve at the sciatic notch (proximal), compound muscle action potentials (CMAPs) were recorded at the hind paw muscles using steel needle electrodes. Distal and proximal latencies as well as the distance between stimulation sites were measured. The corresponding nerve conduction velocity (NCV) was calculated by the distance between stimulation sites divided by the difference between proximal and distal latencies. Moreover, F wave latencies and F wave persistence at different stimulation intervals (1 Hz, 10 Hz) were recorded. All neurographic recordings were performed with a digital Neurosoft-Evidence 3102 electromyograph (Schreiber & Tholen Medizintechnik).

2.7. Motor performance tests

Grip strength of the hindlimbs was measured using an automated Grip Strength Meter (Columbus Instruments) as described previously [23]. With forelimbs supported by a metal grid, mice were trained to hold a grip bar properly with hind paws. The maximum force (in newton) was measured when the mouse was pulled off the grip bar with constant strength. Ten measurements per day were performed on 3 consecutive days and the mean of the measurements was calculated.

To determine motor deficits mice were placed on a rod from a RotaRod Advanced System (TSE Systems) as described previously [23] and were trained to walk on the accelerating rod (5–50 rpm; max latency: 300 s) until falling off. 5 training runs were performed on 2

consecutive days and the latency to fall was measured for 5 runs on the third day.

2.8. Statistical analysis

All experiments were performed with the investigators blinded and unaware of the genotype and the treatment status of the analyzed animals. No significant differences between Cx32def males and females were observed at the investigated time points, confirming previous observations by our group [17] and others [18]. Therefore, male hemizygous and female homozygous mice were grouped together, and the genotypes were indicated as Cx32def (including Cx32-/Y and Cx32-/-). Animals were randomly placed into experimental or control groups according to genotyping results using a random generator (http://www.randomizer.org). Biometrical sample size estimation was performed with G*Power [24]. Calculation of sample appropriate size groups was performed using an a priori power analysis with a defined adequate power of 0.8 (1 - beta error) and an α error of 0.05. To determine the prespecified effect size d, previously published data were considered as comparable reference values [21,23]. Data sets were tested for normal distribution and variance homology. Normally distributed data was further analyzed by one-way ANOVA and the Tukey's multiple comparison test, not normally distributed data was analyzed by Kruskal-Wallis and Dunn's multiple comparisons test. Multiple comparison tests were conducted across all groups, except for morphological analysis (Fig. 5), where only Cx32def mice (control and FTY720 treated) were statistically compared without WT groups, as indicated in the respective figure legends. Significance levels (* $p < 0.05$, ** $p < 0.01$, *** $p < 0.001$) and statistical tests are indicated together in the figure legends. A robust power value (>0.8) of most of the significant results was validated in individual post-hoc power analysis between Cx32def mutant groups and calculations are available upon reasonable request. Measurements and quantifications are shown as individual values (n-numbers are represented in the graphs as circles) and mean ± SD, unless stated otherwise. Sample sizes differed between immunohistochemical ($n = 4$–8), morphological ($n = 5$–10) and functional analysis ($n = 9$–11). Males and females were equally represented across groups whenever possible; however, in groups with an odd sample size, sex distribution differed by one animal. All statistical analyses and generation of graphs were performed with GraphPad Prism (Version 8).

3. Results

3.1. FTY720 treatment prevents T cell recruitment in femoral quadriceps nerves and ventral spinal roots of Cx32def mice

In order to investigate the therapeutic potential of fingolimod (FTY720) in ameliorating the pathology in CMT1X, mice deficient for Cx32 (Cx32def) were treated from 3 months of age to 12 months of age. FTY720 had no impact on body weight, as no significant weight difference was detectable between wild-type (WT) mice and treated or untreated Cx32def mutants at the end of the study (WT = 32.9 g; Cx32def Ctrl = 30.4 g; Cx32def FTY720 = 29.8 g). To characterize the effect of the treatment in the peripheral nervous system, we primarily focused on femoral quadriceps nerves, a well-characterized compartment that reflects the pathology in this mouse model. As demonstrated in previous studies [3,7], the number of CD8+ T-lymphocytes was significantly higher in peripheral nerves of 12-month-old Cx32def mice compared to wild-type mice, with CD8+ T-lymphocytes outnumbering CD4+ T-lymphocytes in peripheral nerves (Fig. 1A-D). After 9 months of FTY720 treatment, however, a robust decline of the CD8+ and CD4+ T-lymphocytes in quadriceps nerves of Cx32def mice was observed, demonstrating the efficacy of this immunomodulatory drug. Similar observations were gained in the ventral spinal roots of Cx32def mice, where FTY720 treatment also prevented the significant increase in the number of CD8+ and CD4+ T-lymphocytes in Cx32def def control compared to WT mice (Fig. 1E-H). These results indicate that FTY720 treatment efficiently prevented the recruitment and colonization of T-lymphocytes in the peripheral nervous system of Cx32def mice.

3.2. FTY720 treatment leads to a decline of macrophage numbers in ventral spinal roots but not in femoral quadriceps nerves

As a next step, we investigated whether endoneurial macrophages are affected by the depletion of T-lymphocytes through staining with a pan-macrophage marker, F4/80. In contrast to a previous study focusing on the genetic inactivation of the adaptive immune system [7], reduced numbers of T-lymphocytes in Cx32def mice treated with FTY720 did not lead to a reduction in number of F4/80+ macrophages in femoral quadriceps nerves (Fig. 2A, B). In ventral roots of Cx32def mice, FTY720 treatment resulted in tendentially reduced number of macrophages (Fig. 2C, D). Overall, we found strongly reduced numbers of lymphocytes while macrophages numbers were only partially attenuated by FTY720 treatment in Cx32def mice.

3.3. FTY720 treatment improves distinct clinical parameters of neuropathy

We then assessed whether the partially ameliorated pathology in Cx32def mice after FTY720 treatment was also associated with an improved clinical outcome in this mouse model. In electrophysiological measurements, both distal and proximal compound muscle action potentials (CMAPs) of Cx32def mice treated with FTY720 showed mild trends of elevation compared to untreated Cx32def mice (Fig. 3A, B). Nerve conduction velocity and F wave latency, features predominantly impaired in both mouse models and human patients of CMT1X, were significantly improved in Cx32def mice after FTY720 treatment (Fig. 3C, D). Furthermore, F wave persistence in Cx32def showed significant reduction compared to wild-type mice at 10 Hz, and it was rescued after FTY720 treatment (Fig. 3E, F). Next, we assessed hind limb grip strength and rotarod performance. While no significant decline in strength was observed in Cx32def control mutant compared to WT mice at 3, 6 and 9 months of age (data not shown), measurement of hind limb grip strength revealed that FTY720 also prevented the reduction of grip strength in Cx32def mice at 12 months of age (Fig. 4A), thus going along with the beneficial effects of FTY720 treatment in electrophysiological measurements. Notably, FTY720 treatment did not lead to improved rotarod performance compared to untreated Cx32def mice at 12 months of age, although the reduced latency to fall in Cx32def mice was transiently preserved after FTY720 treatment at 9 months of age (Fig. 4B, C). To summarize, FTY720 treatment in Cx32def mice improved motor performance and preserved muscle strength.

3.4. FTY720 treatment reduces axon damage predominantly in ventral roots

To examine whether the changes in immune cell numbers resulted in altered neuropathy, we investigated both quadriceps nerves and ventral spinal roots of wild-type, Cx32def mice, and Cx32def mice treated with FTY720. In femoral quadriceps nerves, neither the myelin phenotype nor axonal damage observed in Cx32def mice could be ameliorated by the FTY720 treatment (Fig. 5A, B). Correspondingly, the number of myelin phagocytosing macrophages was also not altered in Cx32def mice treated by FTY720 compared to untreated Cx32def mice (Fig. 5C).

In contrast, ventral spinal roots of Cx32def mice treated by FTY720 presented significantly fewer abnormally myelinated axons (Fig. 5D, G). However, this improved myelin integrity was not reflected by any change in number of phagocytosing macrophages in the ventral roots of Cx32def mice treated with FTY720 (Fig. 5F). Interestingly, axonal damage in Cx32def mice was also substantially reduced after FTY720 treatment (Fig. 5E, G). This shows that FTY720 treatment can improve nerve structure in ventral roots, but not femoral quadriceps nerves.

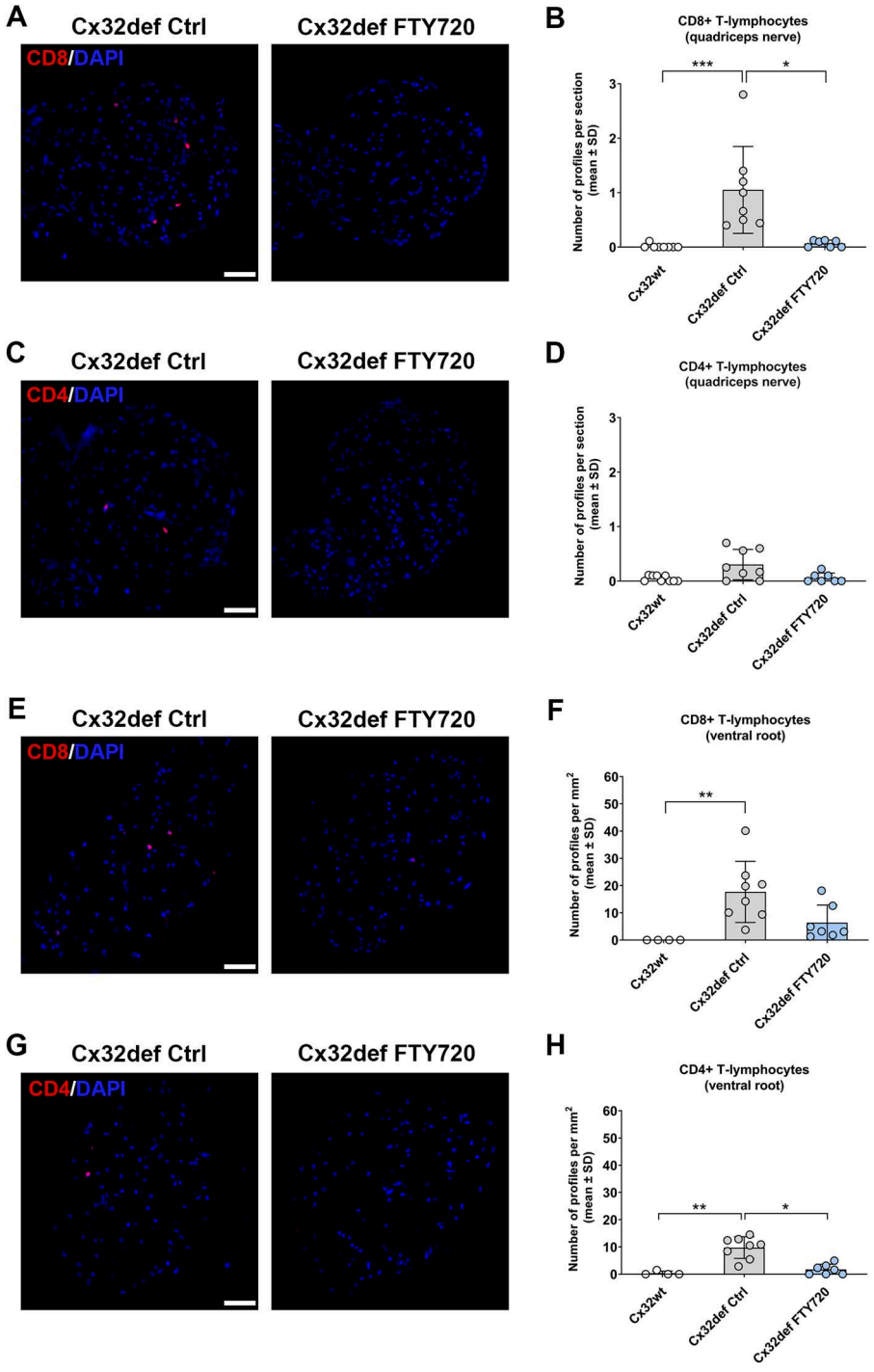

Fig. 1. Fingolimod (FTY720) treatment prevents the recruitment and colonization of T-lymphocytes in the PNS of Cx32def mice. (A), (C) Representative micrographs of CD8 (A) and CD4 (C) immunoreactivity (red) in cross-sections of femoral quadriceps nerves reveals of 12-month-old Cx32def Ctrl (left) and FTY720 treated Cx32def mice (right). Nuclei are labelled with DAPI. Scale bar = 50 μm. (B) – (D) Corresponding quantification of CD8- (B) and CD4-positive (D) profiles in femoral quadriceps nerves reveals an increase in the number of T-lymphocytes in 12-month-old Cx32def control mice compared to Cx32wt mice. FTY720 treatment prevents the recruitment of T-lymphocytes thus, resulting in lower numbers of CD8- (B) and CD4-positive (D) profiles. Kruskal-Wallis and Dunn's post hoc tests; * $p < 0.05$; *** $p < 0.001$. (E), (G) Representative micrographs of CD8 (E) and CD4 (G) immunoreactivity (red) in cross-sections of lumbar ventral roots reveals of 12-month-old Cx32def Ctrl (left) and FTY720 treated Cx32def mice (right). Nuclei are labelled with DAPI. Scale bar = 50 μm. (F) – (H) Corresponding quantification of CD8- (F) and CD4-positive (H) profiles per mm^2 in lumbar ventral roots reveals a significant increase in the number of T-lymphocytes in 12-month-old Cx32def control mice compared to Cx32wt mice. FTY720 treatment results in a robust decrease in the numbers of CD8 (F) and CD4-positive (H) profiles. Kruskal-Wallis and Dunn's post hoc tests; * $p < 0.05$; ** $p < 0.01$. (For interpretation of the references to colour in this figure legend, the reader is referred to the web version of this article).

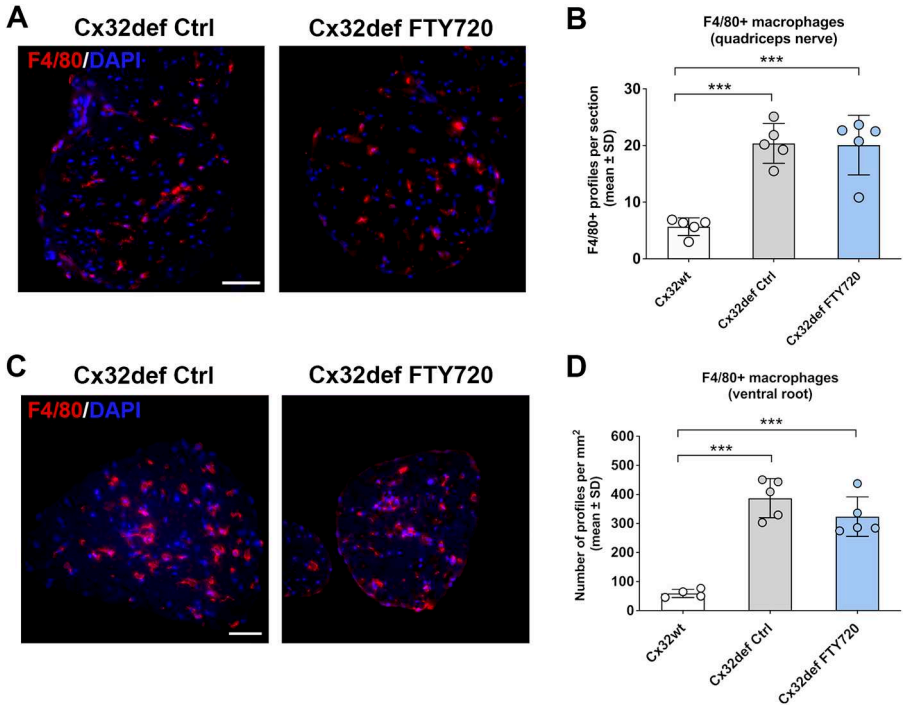

Fig. 2. Fingolimod (FTY720) treatment leads to mildly reduced macrophage numbers only in ventral spinal roots of Cx32def mice. (A) Representative micrographs of F4/80 immunoreactivity (red) in cross-sections of femoral quadriceps nerves of 12-month-old Cx32def Ctrl (left) and FTY720 treated Cx32def mice (right). Nuclei are labelled with DAPI. Scale bar = 50 μm. (B) Corresponding quantification of F4/80-positive profiles reveals a significant increase of macrophage numbers in Cx32def mutant groups compared to Cx32wt mice. FTY720 treatment does not alter the number of macrophages. One-way ANOVA and Tukey's post hoc tests; *** $p < 0.001$. (C) Representative micrographs of F4/80 immunoreactivity (red) in cross-sections of lumbar ventral roots reveals of 12-month-old Cx32def Ctrl (left) and FTY720 treated Cx32def mice (right). Nuclei are labelled with DAPI. Scale bar = 50 μm. (D) Corresponding quantification of F4/80-positive profiles per mm² in lumbar ventral roots reveals a significant increase of macrophage numbers in Cx32def mutant groups compared to Cx32wt mice. FTY720 treatment leads to a non-significant decline in the number of macrophages. One-way ANOVA and Tukey's post hoc tests; *** $p < 0.001$. (For interpretation of the references to colour in this figure legend, the reader is referred to the web version of this article).

4. Discussion

Based on our previous finding that genetic inactivation of the adaptive immune system - by crossbreeding CMT models with RAG1-deficient mice lacking T- and B-lymphocytes -ameliorates CMT1X neuropathy in the respective mouse model [7], we tested the possibility whether pharmacological targeting of T-lymphocyte trafficking may lead to a similar disease-mitigating effect. As a translational approach, we selected FTY720 as a therapeutic immune modulator that is in clinical use for treatment of multiple sclerosis with well-defined site effects and safety requirements, even in children [9,25,26].

We found that treatment with FTY720 indeed leads to reduced numbers of CD8+ and CD4+ T-lymphocytes in both femoral quadriceps nerve as well as in ventral spinal roots, comparable to observations in RAG1-deficient Cx32def mutants displaying mitigated neuropathy [7]. Although not strictly proven by our present studies, it is plausible to assume that the improved histopathological features in ventral roots and functional/clinical amelioration reflect the reduced impact of the adaptive immune system of the treated mouse models. Interestingly, and in full agreement with our present data, the genetic inactivation of the adaptive immune system in distinct CMT1 mutant mice (i.e., Cx32def and P0het) through RAG1-deficiency also led to a stronger amelioration of the neuropathy in ventral roots compared to femoral quadriceps nerves [7,27]. In this context, we speculate that CD8+ cytotoxic T-lymphocytes are the major pathogenic culprits among the adaptive immune system in the CMT1X model. First, CD8+ T-lymphocytes are the most abundant adaptive immune cells in peripheral nerves of CMT1X, but also CMT1B models, outnumbering CD4+ cells by far [7,27,28]. However, studies with CD8-deficient mice or bone marrow chimera approaches implicating mutants deficient in distinct cytotoxic effector molecules (i.e., perforin or granzyme B) [11,29] would be necessary to unequivocally proof a direct CD8-mediated nerve toxicity. Of note, using bone marrow chimera approaches in models of other genetically mediated CNS diseases and in normal aging, CD8+ cells have unequivocally been identified as pathogenic, by attacking oligodendrocytic myelin [11, 29–31].

While macrophages of the ventral spinal roots are also tendentially reduced in numbers upon modulation of the adaptive immune system - possibly reflecting corresponding observations in RAG1-deficient CMT models and suggesting a potential role for T-lymphocytes in macrophage recruitment [7,27] - macrophage numbers in quadriceps nerves remained at a higher level. The reasons underlying this unexpected observation are not clear. It is possible that macrophages from nerves and roots may differ regarding their potential interactions with the adaptive immune system. Of note, the peri-/epineurial compartment of peripheral nerves could contribute to the origin of nerve macrophages [32–34]. Assuming nerve sheaths as possible source of macrophages, and considering the different architecture of these structures in peripheral nerves versus spinal roots [35,36], it is plausible to assume that the corresponding compartments may generate distinct subsets of macrophages possibly explaining the observed differences upon treatment. The relationship between T-lymphocytes and macrophage recruitment is complex, and the specific mechanisms by which T-lymphocytes might interact with macrophages in CMT1 remain unclear. Previous studies in the PNS have described the attraction and activation of macrophages by T-lymphocyte-derived cytokines [37] and similar interactions are reported for microglia and T-lymphocytes in the CNS [38–40]. However, direct mechanistic evidence for this interaction in peripheral nerves of Cx32def mice is still lacking and should be explored in future studies. Independent from these considerations, the reduction

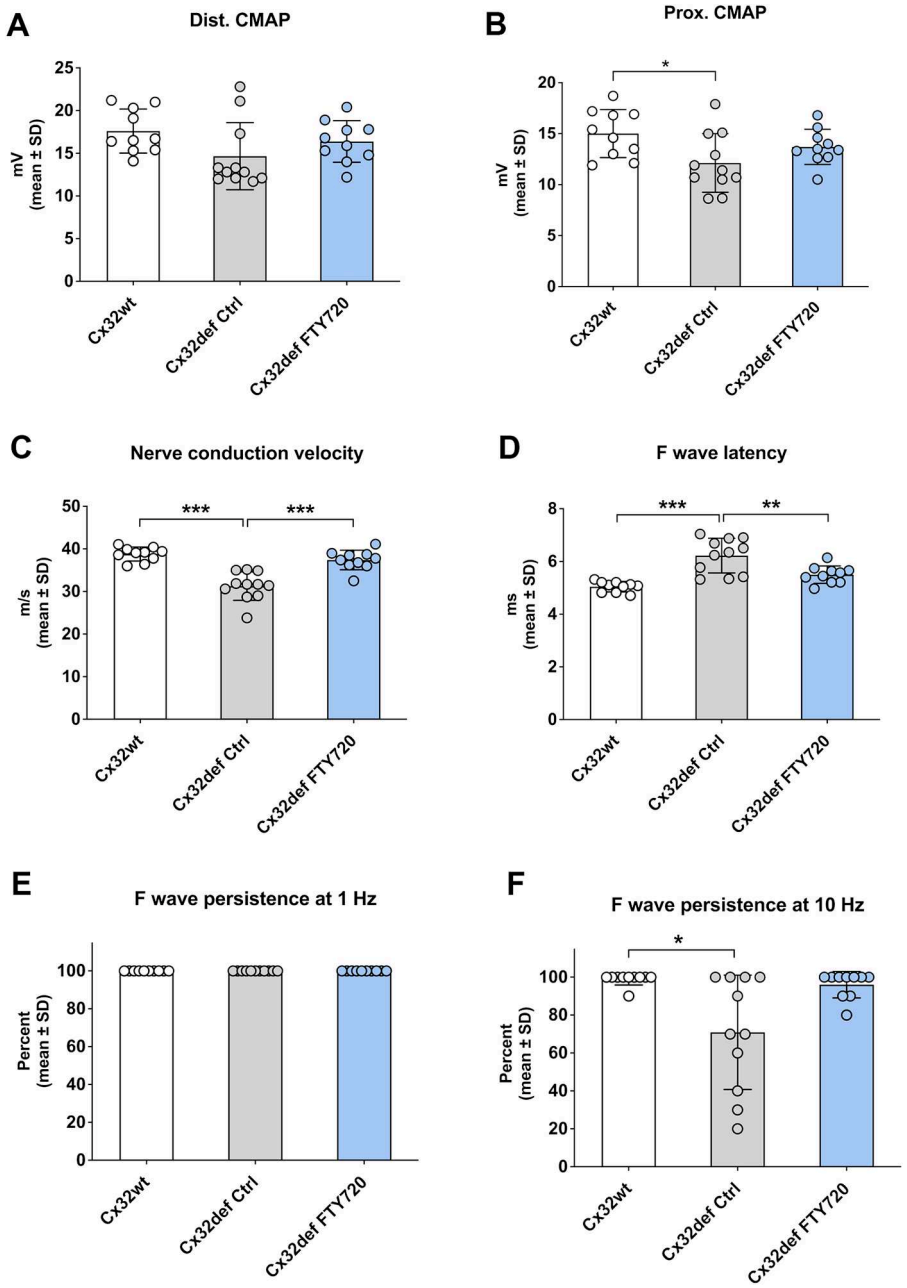

Fig. 3. Fingolimod (FTY720) treatment improves nerve function in Cx32def mice. (A) – (D) Quantification of distal (A) and proximal (B) compound muscle action potentials (CMAP) amplitudes, nerve conduction velocity (NCV, C) and F wave latency (D) of 12-month-old mice. Cx32def control mice are affected by a reduction in distal (A) and proximal (B) CMAP amplitudes, NCV (C), as well as an increased F wave latency (D) compared to Cx32wt mice. FTY720 treatment prevents the decline of these neurographic parameters in Cx32def mice (A – D). One-way ANOVA and Tukey's post hoc tests; * $p < 0.05$; ** $p < 0.01$; *** $p < 0.001$. (E) – (F) Quantification of F wave persistence at 1 Hz (E) and 10 Hz (F) stimulation. At 1 Hz, F wave persistence is unchanged in FTY720 treated and Cx32def control mice in comparison to Cx32wt mice (E). At a higher, more challenging stimulation frequency (10 Hz), F wave persistence is significantly reduced in Cx32def control mice, but fully rescued by FTY720 treatment. Kruskal-Wallis and Dunn's post hoc tests; * $p < 0.05$.

of macrophages by FTY720 treatment in spinal roots, but not in nerves, may be related to the improved histopathological features solely observed in ventral roots, emphasizing the previously identified pathogenic impact of the innate immune system in CMT1 models [1].

Regarding the positive effects of FTY720 on the diseased or damaged nervous system, the drug has been reported to exert additional pleiotropic functions independently from the immune system [41], which may also play a role in the beneficial outcomes observed in our study. Regarding the peripheral nervous system, in vitro studies revealed that FTY720 fosters the transition from Schwann cells into repair/Büngner cells and the secretion of neurite-outgrowth-promoting molecules [42, 43], being in line with the observation that FTY720-treated mice show increased axonal regeneration after nerve injury [44–46]. The possibility that FTY720 may improve nerve function and clinical outcome independently from the adaptive immune system is of particular relevance for CMT1A models (and likely the respective human disease) as we previously showed that in these models the neuropathic features develop independently of the adaptive immune system [47]. Thus, improving axonopathic features and clinical outcome by treating CMT1A models with FTY720 would argue in favour of beneficial mechanisms of the drug independent of the adaptive immune system.

Apparently, the histopathological improvement in ventral roots by

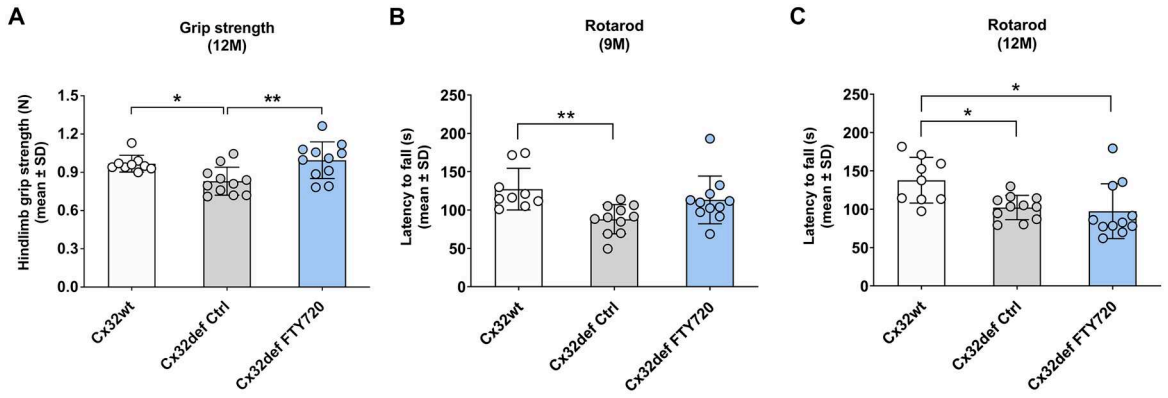

Fig. 4. Fingolimod (FTY720) treatment preserves grip strength in Cx32def mice. (A) Analysis of hind limb grip strength in 12-months-old mice reveals a significant reduction of strength in Cx32def control mice compared to Cx32wt mice. FTY720 treatment prevents the loss of hind limb grip strength in Cx32def mice. One-way ANOVA and Tukey' post hoc tests; * $p < 0.05$; ** $p < 0.01$. (B) – (C) Longitudinal analysis of rotarod performance (latency to fall) in 9 (B) and 12-month-old mice (C) demonstrates a significant reduction in latency to fall in Cx32def control mice compared to Cx32wt mice at 9 and at 12 months. FTY720 treatment transiently attenuates rotarod impairment in Cx32def mice (B). One-way ANOVA and Tukey' post hoc tests; ** $p < 0.01$.

FTY720 treatment may cause the better clinical outcome observed. For instance, F wave latency significantly improved upon treatment. Even more striking was the F wave persistence upon challenging the nerve by increased stimulation frequency: while at 1 Hz, there was a constant F wave response in normal WT, untreated and treated Cx32def mutants, we found in untreated Cx32def mutants a robust decline in F wave persistence by 30 % when stimulation frequency was increased to 10 Hz. Notably, this decline was fully corrected by FTY720 treatment, likely reflecting beneficial effects on motor neuron excitability and axon damage. Why the preserved NCV was not reflected by morphological improvements in distal nerves remains enigmatic. In fact, this was not the first observation showing an "uncoupling" of axonal properties, clinical outcome and morphological alterations [3,21]. It is conceivable that modifying parameters of the NCV may not only be related to demyelination but also to altered distribution of ion channels [48–50]; this issue has not been addressed here as this is out of the scope of the study. Thus, it is possible that the improvement in NCV in the absence of an amelioration of pathological features is related to molecular alterations of diseased nerve fibers (e.g., distribution of ion channels).

Finally, clinical parameters were significantly improved upon FTY720 treatment. Rotarod performance, representing an overall motor behavior, was improved upon FTY720 treatment at 9 months of age and comparable to WT mice, as reflected by a preserved latency to fall. It is presently not known why this beneficial effect persists only transiently. Muscle strength, a leading clinical issue of CMT1X patients [51], was generally rescued by FTY720 treatment. In longitudinal measurements of grip strength, 9-month-old untreated Cx32def mice showed mild deterioration of grip strength in comparison to WT mice (data not shown). This mild reduction was not influenced by FTY720 treatment. However, at 12 months of age, untreated Cx32-deficient mice experienced a further decline in grip strength, which was prevented by FTY720 treatment, thus reflecting the overall improvement of grip strength at 12 months.

One potential limitation of the Cx32def mouse model used in our study is that most disease-causing mutations are missense variants, while the complete deletion of *GJB1* is rare among CMT1X patients [52,53]. However, several in vivo models have shown that Cx32 mutants exhibit a loss of function without toxic effects [54–56]. This is confirmed by clinical observations indicating that CMT1X patients exhibit similar disease phenotypes and progression regardless of their mutation, suggesting that loss of function is the detrimental mechanism driving the peripheral manifestations of the disorder [51,52,57]. Emphasizing the overarching role of inflammation in CMT1X models and likely in the human disease, macrophage activation has been demonstrated in other mouse models expressing CMT1X mutations [56,58]. Future studies are needed to confirm whether FTY720 treatment is also beneficial in these CMT1X mouse models.

Nevertheless, we believe that our findings may have potential translational implications. Although FTY720 treatment leads to well-known side effects like lymphopenia [9,25], our data may suggest a potentially clinical use, especially in severe cases of CMT1X, possibly driven by a particularly robust neuroinflammation [59,60]. Indeed, previous studies of our laboratory recommended off-label approaches of FTY720 in severe, genetically mediated childhood diseases of the CNS [12,61], which indeed are now translated into compassionate use of the drug (Goy, Martini and Rostasy, unpublished data). Given the well-known safety profile of FTY720 and after thoroughly weighing its advantages and disadvantages, it is reasonable to consider that the drug might be effective in severe cases of CMT1X to mitigate disease burden. Ideally, targeting the adaptive immune system with novel drugs with preferentially mild side effects could be combined with other approaches, like physical exercise which is not only beneficial for health and well-being in general, but may additionally mitigate neuropathy, as previously shown in CMT1X models [21,23].

5. Conclusion

We previously observed that the neuropathy is substantially ameliorated in a CMT1X model when the adaptive immune system is genetically depleted. Here, we tried to translate these findings by pharmacologically suppressing lymph node emigration of lymphocytes by the sphingosine-1-phosphate receptor modulator FTY720. Upon treatment, certain histopathological, electrophysiological and clinical parameters were improved. We conclude that the approved immune modulator FTY720 can dampen neuropathic features in CMT1X models. Therefore, targeting the adaptive immune system in general may be a therapeutic option for CMT1X.

CRediT authorship contribution statement

Xidi Yuan: Writing – original draft, Methodology, Investigation, Formal analysis, Data curation. **Dennis Klein:** Writing – review & editing, Writing – original draft, Supervision, Methodology, Investigation, Formal analysis, Data curation, Conceptualization. **Anna-Maria Maier:** Methodology, Investigation, Formal analysis. **Rudolf Martini:** Writing – review & editing, Supervision, Project administration, Data curation, Conceptualization.

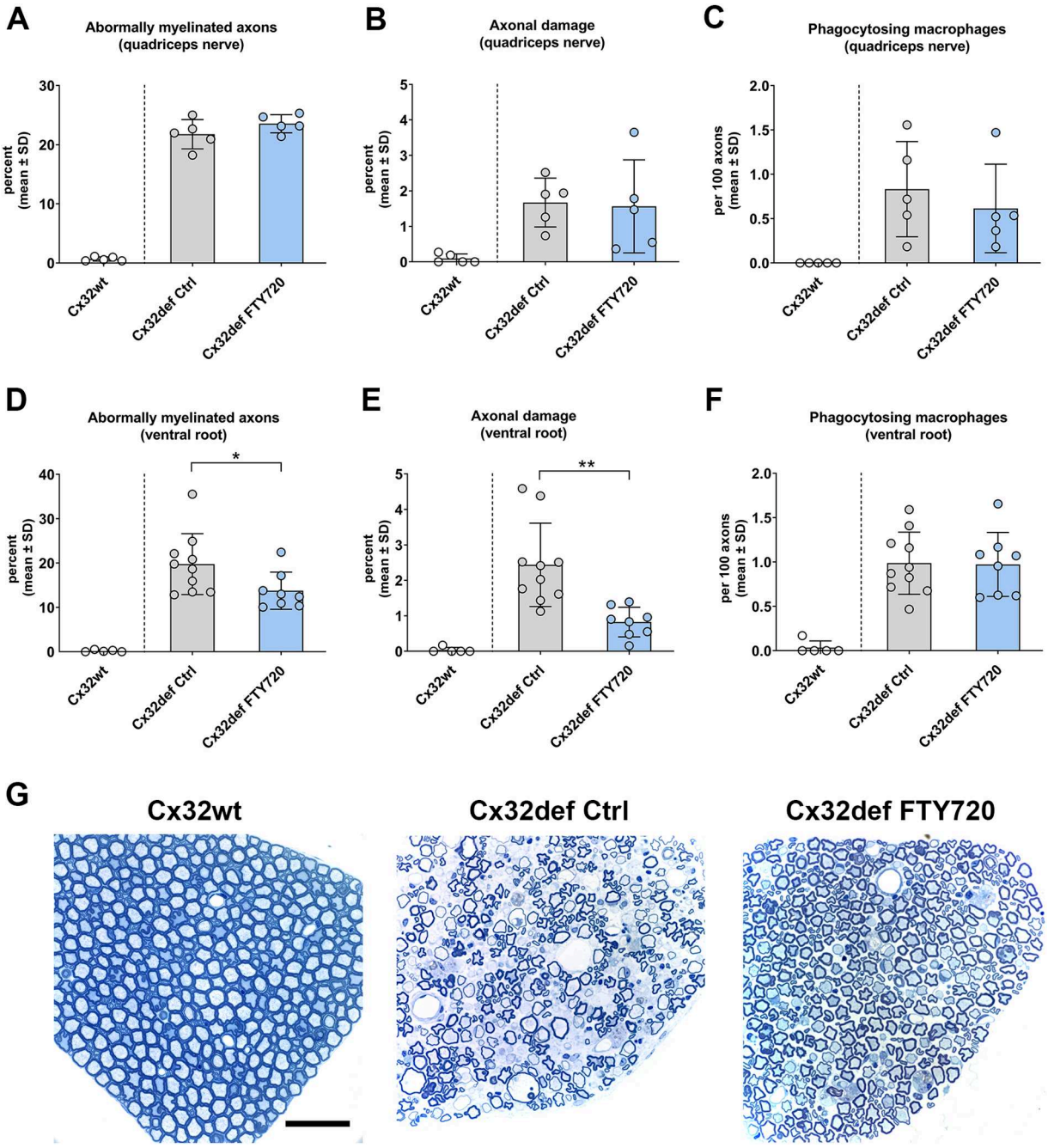

Fig. 5. Fingolimod (FTY720) treatment attenuates peripheral neuropathy only in ventral spinal roots of Cx32def mice. (A) - (C). Quantification of abnormally (de- and thinly) myelinated fibers (A), axon damage (B) and phagocytosing macrophages (C) in femoral quadriceps nerves. FTY720 treatment has no impact on their frequency in Cx32def mutants. (D) - (F). Quantification of abnormally (de- and thinly) myelinated fibers (D), axon damage (E) and phagocytosing macrophages (F) in lumbar ventral roots. FTY720 treatment significantly mitigates the frequency of abnormally myelinated fibers (D) and axonopathic profiles (E) in Cx32def mice, whereas the number of phagocytosing macrophages is not altered upon treatment (F). For electron microscopic analysis only Cx32def mutant mice were compared statistically, as indicated by the black dashed line. Pathological alterations are barely detectable in Cx32wt mice. Two-tailed Student's *t*-test; * $p < 0.05$; ** $p < 0.01$. (G) Representative semithin sections of lumbar ventral roots of 12-months-old Cx32wt (left) Cx32def Ctrl (middle) and FTY720 treated Cx32def mice (right). Scale bar = 50 μm.

Declaration of competing interest

None of the authors reports disclosures relevant to the manuscript.

Study funding

The study was supported by Therapies for Inherited Neuropathies (TIN), the Elite Network of Bavaria "Translational Neuroscience" and German Research Foundation (DFG, MA 1053/7–1).

Acknowledgements

The authors are grateful to Heinrich Blazyca, Silke Loserth and Bettina Meyer for expert technical assistance and to Anja Weidner and Thomas Bimmerlein for attentive animal care. We thank Janos Groh and Michaela Hörner for discussions and suggestions.

Abbreviations

BSA, Bovine serum albumin; CMAP, Compound muscle action potential; CMT, Charcot-Marie-Tooth type; CMT1X, X-linked dominant form of CMT1; CNS, Central nervous system; CSF-1, Colony stimulating factor 1; Ctrl, Control; FTY720, Fingolimod; NCV, Nerve conduction velocity; PBS, Phosphate-buffered saline; PNS, Peripheral nervous system; S1PR, Sphingosine-1-phosphate receptor; WT, Wild-type.

Data availability

The data that support the findings of this study are available from the corresponding author upon reasonable request.

References

[1] Klein D, Martini R. Myelin and macrophages in the PNS: an intimate relationship in trauma and disease. Brain Res 2016;1641:130–8.
[2] Bolino A, D'Antonio M. Recent advances in the treatment of Charcot-Marie-Tooth neuropathies. J Peripher Nerv Syst 2023;28:134–49.
[3] Klein D, Patzko A, Schreiber D, van Hauwermeiren A, Baier M, Groh J, et al. Targeting the colony stimulating factor 1 receptor alleviates two forms of Charcot-Marie-Tooth disease in mice. Brain: J Neurol 2015;138:3193–205.
[4] Klein D, Groh J, Yuan X, Berve K, Stassart R, Fledrich R, et al. Early targeting of endoneurial macrophages alleviates the neuropathy and affects abnormal Schwann cell differentiation in a mouse model of Charcot-Marie-Tooth 1A. Glia 2022;70:1100–16.
[5] Ostertag C, Klein D, Martini R. Presymptomatic macrophage targeting has a long-lasting therapeutic effect on treatment termination in a mouse model of Charcot-Marie-Tooth 1. Exp Neurol 2022;357:114195.
[6] Groh J, Klein I, Hollmann C, Wettmarshausen J, Klein D, Martini R. CSF-1-activated macrophages are target-directed and essential mediators of schwann cell dedifferentiation and dysfunction in Cx32-deficient mice. Glia 2015;63:977–86.
[7] Kobsar I, Berghoff M, Samsam M, Wessig C, Maurer M, Toyka KV, et al. Preserved myelin integrity and reduced axonopathy in connexin32-deficient mice lacking the recombination activating gene-1. Brain 2003;126:804–13.
[8] Melzer N, Meuth SG. Disease-modifying therapy in multiple sclerosis and chronic inflammatory demyelinating polyradiculoneuropathy: common and divergent current and future strategies. Clin Exp Immunol 2014;175:359–72.
[9] Meuth SG, Gobel K, Wiendl H. Immune therapy of Multiple sclerosis - future strategies. Curr Pharm Des 2012.
[10] Brinkmann V, Billich A, Baumruker T, Heining P, Schmouder R, Francis G, et al. Fingolimod (FTY720): discovery and development of an oral drug to treat multiple sclerosis. Nat Rev Drug Discov 2010;9:883–97.
[11] Abdelwahab T, Stadler D, Knopper K, Arampatzi P, Saliba AE, Kastenmuller W, et al. Cytotoxic CNS-associated T cells drive axon degeneration by targeting perturbed oligodendrocytes in PLP1 mutant mice. iScience 2023;26:106698.
[12] Groh J, Berve K, Martini R. Fingolimod and teriflunomide attenuate neurodegeneration in mouse models of neuronal ceroid lipofuscinosis. Mol Ther 2017;25:1889–99.
[13] Groh J, Berve K, Martini R. Immune modulation attenuates infantile neuronal ceroid lipofuscinosis in mice before and after disease onset. Brain Commun 2021;3:fcab047.
[14] Horner M, Groh J, Klein D, Ilg W, Schols L, Dos Santos S, et al. CNS-associated T-lymphocytes in a mouse model of Hereditary Spastic Paraplegia type 11 (SPG11) are therapeutic targets for established immunomodulators. Exp Neurol 2022;355:114119.
[15] Anzini P, Neuberg DH, Schachner M, Nelles E, Willecke K, Zielasek J, et al. Structural abnormalities and deficient maintenance of peripheral nerve myelin in mice lacking the gap junction protein connexin 32. J Neurosci: Offic J Society Neurosci 1997;17:4545–51.
[16] Nelles E, Butzler C, Jung D, Temme A, Gabriel HD, Dahl U, et al. Defective propagation of signals generated by sympathetic nerve stimulation in the liver of connexin32-deficient mice. Proc Natl Acad Sci U S A 1996;93:9565–70.
[17] Groh J, Heinl K, Kohl B, Wessig C, Greeske J, Fischer S, et al. Attenuation of MCP-1/CCL2 expression ameliorates neuropathy in a mouse model for Charcot-Marie-Tooth 1X. Hum Mol Genet 2010;19:3530–43.
[18] Kagiava A, Richter J, Tryfonos C, Karaiskos C, Heslegrave AJ, Sargiannidou I, et al. Gene replacement therapy after neuropathy onset provides therapeutic benefit in a model of CMT1X. Hum Mol Genet 2019;28:3528–42.
[19] Groh J, Basu R, Stanley ER, Martini R. Cell-surface and secreted isoforms of CSF-1 exert opposing roles in macrophage-mediated neural damage in Cx32-deficient mice. J Neurosci: Offic J Society Neurosci 2016;36:1890–901.
[20] Yuan X, Klein D, Kerscher S, West BL, Weis J, Katona I, et al. Macrophage depletion ameliorates peripheral neuropathy in aging mice. J Neurosci: Offic J Society Neurosci 2018;38:4610–20.
[21] Klein D, Yepez MG, Martini R. Physical exercise halts further functional decline in an animal model for Charcot-Marie-Tooth disease 1X at an advanced disease stage. J Peripher Nerv Syst 2024.
[22] Zielasek J, Martini R, Toyka KV. Functional abnormalities in P0-deficient mice resemble human hereditary neuropathies linked to P0 gene mutations. Muscle Nerve 1996;19:946–52.
[23] Klein D, Yuan X, Weiss EM, Martini R. Physical exercise mitigates neuropathic changes in an animal model for Charcot-Marie-Tooth disease 1X. Exp Neurol 2021;343:113786.
[24] Faul F, Erdfelder E, Lang AG, Buchner A. G*Power 3: a flexible statistical power analysis program for the social, behavioral, and biomedical sciences. Behav Res Methods 2007;39:175–91.
[25] Gonzalez-Lorenzo M, Ridley B, Minozzi S, Del Giovane C, Peryer G, Piggott T, et al. Immunomodulators and immunosuppressants for relapsing-remitting multiple sclerosis: a network meta-analysis. Cochrane Database Syst Rev 2024;1:CD011381.
[26] Chitnis T, Arnold DL, Banwell B, Bruck W, Ghezzi A, Giovannoni G, et al. Trial of Fingolimod versus Interferon beta-1a in pediatric Multiple sclerosis. N Engl J Med 2018;379:1017–27.
[27] Schmid CD, Stienekemeier M, Oehen S, Bootz F, Zielasek J, Gold R, et al. Immune deficiency in mouse models for inherited peripheral neuropathies leads to improved myelin maintenance. J Neurosci: Offic J Society Neurosci 2000;20:729–35.
[28] Mäurer M, Schmid CD, Bootz F, Zielasek J, Toyka KV, Oehen S, et al. Bone marrow transfer from wild type mice reverts the beneficial effect of genetically-mediated immune deficiency in myelin mutants. Mol Cell Neurosci 2001;17:1094–101.
[29] Groh J, Knopper K, Arampatzi P, Yuan X, Losslein L, Saliba AE, et al. Accumulation of cytotoxic T cells in the aged CNS leads to axon degeneration and contributes to cognitive and motor decline. Nat Aging 2021;1:357–67.
[30] Groh J, Abdelwahab T, Kattimani Y, Horner M, Loserth S, Gudi V, et al. Microglia-mediated demyelination protects against CD8(+) T cell-driven axon degeneration in mice carrying PLP defects. Nat Commun 2023;14:6911.
[31] Groh J, Martini R. Neuroinflammation as modifier of genetically caused neurological disorders of the central nervous system: understanding pathogenesis and chances for treatment. Glia 2017;65:1407–22.
[32] Ydens E, Amann L, Asselbergh B, Scott CL, Martens L, Sichien D, et al. Profiling peripheral nerve macrophages reveals two macrophage subsets with distinct localization, transcriptome and response to injury. Nat Neurosci 2020;23:676–89.
[33] Wang PL, Yim AKY, Kim KW, Avey D, Czepielewski RS, Colonna M, et al. Peripheral nerve resident macrophages share tissue-specific programming and features of activated microglia. Nat Commun 2020;11:2552.
[34] Kolter J, Kierdorf K, Henneke P. Origin and differentiation of nerve-associated macrophages. J Immunol 2020;204:271–9.
[35] Pettersson CA. Sheaths of the spinal nerve roots. Permeability and structural characteristics of dorsal and ventral spinal nerve roots of the rat. Acta Neuropathol 1993;85:129–37.
[36] Kaar GF, Fraher JP. The sheaths surrounding the attachments of rat lumbar ventral roots to the spinal cord: a light and electron microscopical study. J Anat 1986;148:137–46.
[37] Gold R, Archelos JJ, Hartung H-P. Mechanisms of immune regulation in the peripheral nervous system. Brain Pathol 1999;9:343–60.
[38] Schetters STT, Gomez-Nicola D, Garcia-Vallejo JJ, Van Kooyk Y. Neuroinflammation: Microglia T Cells Get Ready Tango. Front Immunol 2017;8:1905.
[39] Groh J, Ribechini E, Stadler D, Schilling T, Lutz MB, Martini R. Sialoadhesin promotes neuroinflammation-related disease progression in two mouse models of CLN disease. Glia 2016;64:792–809.
[40] Ip CW, Kroner A, Crocker PR, Nave KA, Martini R. Sialoadhesin deficiency ameliorates myelin degeneration and axonopathic changes in the CNS of PLP overexpressing mice. Neurobiol Dis 2007;25:105–11.
[41] Hunter SF, Bowen JD, Reder AT. The direct effects of Fingolimod in the Central nervous system: implications for relapsing multiple sclerosis. CNS Drugs 2016;30:135–47.
[42] Heinen A, Beyer F, Tzekova N, Hartung HP, Kury P. Fingolimod induces the transition to a nerve regeneration promoting Schwann cell phenotype. Exp Neurol 2015;271:25–35.
[43] Schira J, Heinen A, Poschmann G, Ziegler B, Hartung HP, Stuhler K, et al. Secretome analysis of nerve repair mediating Schwann cells reveals Smad-dependent trophism. FASEB J 2019;33:4703–15.
[44] Szepanowski F, Derksen A, Steiner I, Meyer Zu Horste G, Daldrup T, Hartung HP, et al. Fingolimod promotes peripheral nerve regeneration via modulation of lysophospholipid signaling. J Neuroinflammation 2016;13:143.
[45] Li C, Yamamoto T, Kanemaru H, Kishimoto N, Seo K. Effects of sphingosine-1-phosphate on the facilitation of peripheral nerve regeneration. Cureus 2024;16:e73784.
[46] Anastasiadou S, Knoll B. The multiple sclerosis drug fingolimod (FTY720) stimulates neuronal gene expression, axonal growth and regeneration. Exp Neurol 2016;279:243–60.
[47] Kohl B, Groh J, Wessig C, Wiendl H, Kroner A, Martini R. Lack of evidence for a pathogenic role of T-lymphocytes in an animal model for Charcot-Marie-Tooth disease 1A. Neurobiol Dis 2010;38:78–84.
[48] Ulzheimer JC, Peles E, Levinson SR, Martini R. Altered expression of ion channel isoforms at the node of Ranvier in P0-deficient myelin mutants. Mol Cell Neurosci 2004;25:83–94.
[49] Groh J, Weis J, Zieger H, Stanley ER, Heuer H, Martini R. Colony-stimulating factor-1 mediates macrophage-related neural damage in a model for Charcot-Marie-Tooth disease type 1X. Brain: J Neurol 2012;135:88–104.
[50] Rosberg MR, Alvarez S, Klein D, Nielsen FC, Martini R, Levinson SR, et al. Progression of motor axon dysfunction and ectopic Na1.8 expression in a mouse model of Charcot-Marie-Tooth disease 1B. Neurobiol Dis 2016;93:201–14.

[51] Shy ME, Siskind C, Swan ER, Krajewski KM, Doherty T, Fuerst DR, et al. CMT1X phenotypes represent loss of GJB1 gene function. Neurology 2007;68:849–55.
[52] Abrams CK, Goman M, Wong S, Scherer SS, Kleopa KA, Peinado A, et al. Loss of coupling distinguishes GJB1 mutations associated with CNS manifestations of CMT1X from those without CNS manifestations. Sci Rep 2017;7:40166.
[53] Kleopa KA, Abrams CK, Scherer SS. How do mutations in GJB1 cause X-linked Charcot-Marie-Tooth disease? Brain Res 2012;1487:198–205.
[54] Abrams CK, Lancaster E, Li JJ, Dungan G, Gong D, Scherer SS, et al. Knock-in mouse models for CMTX1 show a loss of function phenotype in the peripheral nervous system. Exp Neurol 2023;360:114277.
[55] Sargiannidou I, Vavlitou N, Aristodemou S, Hadjisavvas A, Kyriacou K, Scherer SS, et al. Connexin32 mutations cause loss of function in Schwann cells and oligodendrocytes leading to PNS and CNS myelination defects. J Neurosci 2009;29:4736–49.
[56] Tadenev ALD, Hatton CL, Pattavina B, Mullins T, Schneider R, Bogdanik LP, et al. Two new mouse models of Gjb1-associated Charcot-Marie-Tooth disease type 1X. J Peripher Nerv Syst 2023;28:317–28.
[57] Abrams CK, Freidin M. GJB1-associated X-linked Charcot-Marie-Tooth disease, a disorder affecting the central and peripheral nervous systems. Cell Tissue Res 2015;360:659–73.
[58] Kagiava A, Karaiskos C, Richter J, Tryfonos C, Lapathitis G, Sargiannidou I, et al. Intrathecal gene therapy in mouse models expressing CMT1X mutations. Hum Mol Genet 2018;27:1460–73.
[59] Martini R, Toyka KV. Immune-mediated components of hereditary demyelinating neuropathies: lessons from animal models and patients. Lancet Neurol 2004;3:457–65.
[60] Kamińska J, Kochański A. A role of inflammation in Charcot–Marie–Tooth disorders—In a perspective of treatment? Int J Mol Sci 2025;26:15.
[61] Groh J, Berve K, Martini R. Immune modulation attenuates infantile neuronal ceroid lipofuscinosis in mice before and after disease onset. Brain Comm 2021;3.